Aerosol and Air Quality Research, 18: 2728–2740, 2018

ISSN: 1680-8584 print / 2071-1409 online
doi: 10.4209/aaqr.2018.04.0151

Spatiotemporal Variation, Source Analysis, and Health Risk Assessment of Particle-bound PAHs in Urumqi, China

Maimaiti Simayi[1,2], Palida Yahefu[1*], Mengxin Han[1]

[1] *College of Grassland and Environment Sciences, Xinjiang Agricultural University, Urumqi 830052, China*
[2] *College of Environmental Sciences and Engineering, State Key Joint Laboratory of Environmental Simulation and Pollution Control, Peking University, Beijing 100871, China*

ABSTRACT

The purpose of the present study was to evaluate the polycyclic aromatic hydrocarbons (PAHs) in fine ($PM_{2.5}$) and coarse (PM_{10}) particles in five functional areas, namely, the traffic, industrial, residential, commercial, and educational areas, in Urumqi, a megacity in northwest China. Airborne PM_{10} and $PM_{2.5}$ samples were collected from the five areas during heating (November 2015–March 2016) and non-heating (July–September 2016) periods, and 16 priority PAHs (Σ_{16}PAHs) in the samples were quantified and analyzed. Over the study period, the average Σ_{16}PAHs in the PM_{10} and $PM_{2.5}$ were 116.97 ± 41.44 ng m^{-3} and 88.57 ± 31.22 ng m^{-3}, respectively. During the heating period, Σ_{16}PAHs in both of the fractions were more than 2.5 times those during the non-heating period, with the highest values found in the industrial area during the heating period and in the traffic area during the non-heating period. The northern part of the city had more PAH pollution than the southern part. The compositions of the particle-bound PAHs varied temporally and spatially, with 4-ring PAHs contributing more during the heating period than during the non-heating period and with 5- and 6-ring PAHs exhibiting the opposite trend. In addition, 4-ring PAHs contributed more in the industrial area, whereas 5- and 6-ring PAHs contributed more in the traffic area, reflecting the variety of emission sources. Principal component analysis and diagnostic molecular ratios showed that vehicular exhaust was the major source of PAHs during both periods at the traffic and central urban sites, while heavy-duty vehicular emissions and natural gas/biomass/coal combustion emissions dominated in the industrial area. The average Benzo[a]pyrene equivalent toxicity (BaP_{eq}) ranged from 4.4 to 37.9 ng m^{-3}, showing a generally similar spatiotemporal distribution with the Σ_{16}PAHs. The results showed that the lifetime excess cancer risk (LCR) during the heating period was higher than during the non-heating period and that people who lived around the industrial and traffic areas had a higher likelihood of getting lung cancer than residents in other parts of the city.

Keywords: Polycyclic aromatic hydrocarbons; Particulate matter; Spatiotemporal variations; Source apportionment; Health risk.

INTRODUCTION

In the past few years, accompanying rapid development in China, complex air pollution phenomena such as photochemical pollution and haze episodes characterized by high levels of $PM_{2.5}$ (particulate matter with aerodynamic diameter equal to or < 2.5 μm) have frequently occurred in many large cities (Liu *et al.*, 2013; Tao *et al.*, 2014; Fu *et al.*, 2016). Epidemiological and clinical evidence has shown that morbidity and mortality markedly increased in response to exposure to high levels of particulate matter (PM) (Lim *et al.*, 2012). The premature mortality caused by $PM_{2.5}$ reached 1.27 million in China (Apte *et al.*, 2015). The adverse effects of $PM_{2.5}$ on human health are closely related to its essential components, such as heavy metals, organic pollutants, and some water-soluble ions (Gao *et al.*, 2016). Polycyclic aromatic hydrocarbons (PAHs) are well-known major toxic organic constituents of PM, despite the fact that their contribution to PM mass (< 0.1%) is negligible (Chou *et al.*, 2017); therefore, PAHs are one of the most widely studied components.

PAHs in ambient air have gradually become more important because of their persistence, bioaccumulation, and adverse effects on human health, such as their potentially toxic and carcinogenic effects and their mutagenic activity (Guo *et al.*, 2003; Zhang *et al.*, 2016). PAHs with high toxicity in ambient air are primarily absorbed by PM, especially $PM_{2.5}$, and can easily be breathed into the lungs and ingested in the gut, and exposed skin (Liao *et al.*, 2011). Thus, PAHs associated with PM pose a serious threat towards ecology and human health (Bandowe *et al.*, 2014).

* Corresponding author.
E-mail address: muhammadesmayil@pku.edu.cn

Zhang *et al.* (2009) estimated that 1.6% of the lung cancer morbidity in China might be related to the inhalation of PAHs. The PAHs in urban atmospheres are significantly increasing due to the rapid growth of industrial activities, city populations, traffic densities, and low dispersion of atmospheric pollutants (Tan *et al.*, 2005; Masih *et al.*, 2010). The major anthropogenic emission sources of PAHs include coal combustion, vehicle exhaust, straw burning, wood combustion, waste incineration, and industrial production (He *et al.*, 2014). Vehicular emissions are the major contributor to the urban atmosphere, especially in regions where coal was replaced by gas, and most of the PAHs from vehicular exhaust are classified as carcinogens (Teixeira *et al.*, 2011; Ren *et al.*, 2017).

Atmospheric PAH concentrations vary from place to place because of variations in emissions and atmospheric transport (Zhang *et al.*, 2009). Investigations on the spatiotemporal variation of particulate PAHs in China showed that the cities in northern China have much higher concentrations in winter than cities in other parts of the country, indicating a larger influence on human health (Zhang *et al.*, 2009; Wu *et al.*, 2014). The presence of PAHs is a substantial problem in both large and small cities (Sosa *et al.*, 2017). However, studies on atmospheric PAHs are limited in Xinjiang Province, which is known for its vast oil and gas reserves, and it has become the largest energy base in China. Urumqi, a megacity in northwest China, is located in the center of Eurasia, in the middle north of Tianshan Mountain and on the southern margin of Junggar Basin and is the core node in the Silk Road economic area. Urumqi's topography is very complex, surrounded by mountains in the east, west, and south; the north and the middle part are lower in elevation than the south and northeast. Mountainous ranges reduce atmospheric circulation and pollutant diffusion. Moreover, frequently recurring thermal inversion conditions favor the stagnation and accumulation of pollutants. In spite of this, limited research regarding PAHs in aerosols have been conducted for this crucial region or are restricted to a single sampling point in Urumqi (Limu *et al.*, 2013; Ren *et al.*, 2017). This work aims to (1) identify the spatial and temporal variation of PAH concentration in various particle-size fractions; (2) clarify the possible sources of particulate PAHs and distribution patterns at different functional areas and different periods; and (3) assess the carcinogenic risk of PAHs by the inhalation of PM_{10} and $PM_{2.5}$.

MATERIAL AND METHODS

Site Description and Sample Collection

Urumqi (42°45′32″N–44°08′00″N, 86°37′33″E–88°58′24″E) is the political, economic and cultural center of the Xinjiang Uyghur Autonomous Region in China, at the north foot of Tianshan Mountain and on the south edge of Jungger Basin. Its eastern, southern and western sides are surrounded by mountains, with an average elevation of 800 m. The southeastern part is higher than the northwest part, and the north is similar to a bell mouth that is shaped towards the Junggar Basin.

Urumqi has seven districts and one county, with a population of over 3.5 million people living in an area of 14,216 km^2 (Ren *et al.*, 2017). The weather in Urumqi is extremely dry due to its geographical location and continental climate (Yang *et al.*, 2009). Spring and autumn are short while winter and summer are long. Heating is supplied from October 10 until April 10; therefore, this period is called the heating period. In contrast, the period from April 10 to October 10 is called the non-heating period. In the heating period, PM and other pollutants increase in the ambient air because of the burning of fossil fuels (natural gas and heating oil), and the inversion layer. The inversion layer in Urumqi is relatively deep and stable, and it is prone to occur in the winter half of the year (Li *et al.*, 2015). Nine sampling sites were selected based on their different land-use categories, populations, and traffic densities. The sampling location and a brief introduction are illustrated in Fig. 1 and Table S1, respectively.

Ambient PM_{10} and $PM_{2.5}$ samples were collected simultaneously on pre-baked quartz fiber filters (QFFs, Ø = 90 mm, Whatman, UK; baked in an oven at 450°C for 4 h) at all sampling sites during heating (from November 2015 to March 2016) and non-heating (from July to September 2016) periods. A standard medium volume integrated sampler (100 L min^{-1}, Qingdao Laoshan Mechanical Corp., China) was used, with an average sampling period of 24 h. A total of 110 valid samples, 57 in the heating period and 53 in the non-heating period, were collected and analyzed. The procedure of preparing the filters applied the same procedure as Teixeira *et al.* (2011). The samples were sealed and stored in a refrigerator at –4°C and packed in aluminum foil before extraction and analysis. All filters were extracted within 2 weeks of sampling.

Analytical Procedure

Kong *et al.* (2010, 2013) described the extracting procedure and analyzing methods for the $PM_{2.5}$ and PM_{10} filter samples. This paper adopted the same procedure, and the steps were as follows. The filters were extracted by Soxhlet extraction with 100 mL ether and hexane (1+9; v/v). Extraction was concentrated by using a rotary evaporator, purified with a silica gel cleanup technique, and re-concentrated. Finally, the solution volume was condensed to exactly 1 mL under gentle nitrogen flow in a 60°C water bath. Extracts were filtrated by a 0.25 μm filter, transferred into an ampoule bottle and stored in a refrigerator until HPLC analysis. The procedures of sampling, pretreatment, and analysis were completed within one month.

The 16 PAHs were separated and identified by using an HPLC system, equipped with a UV detector (PDA-100 Photodiode Array Detector) from Dionex Corporation, USA. Four wavelengths (220 nm, 230 nm, 254 nm, 290 nm) of the UV detector were selected. The mobile phase consisted of acetonitrile and water, with a flow rate of 1.0 mL min^{-1}. The column temperature was 30°C, and the sample size was 10 μL. A gradient with acetonitrile and water was applied for separation of the analyses, as exhibited in Table S2.

Quality Assurance and Quality Control

The quantification of PAHs was based on the retention

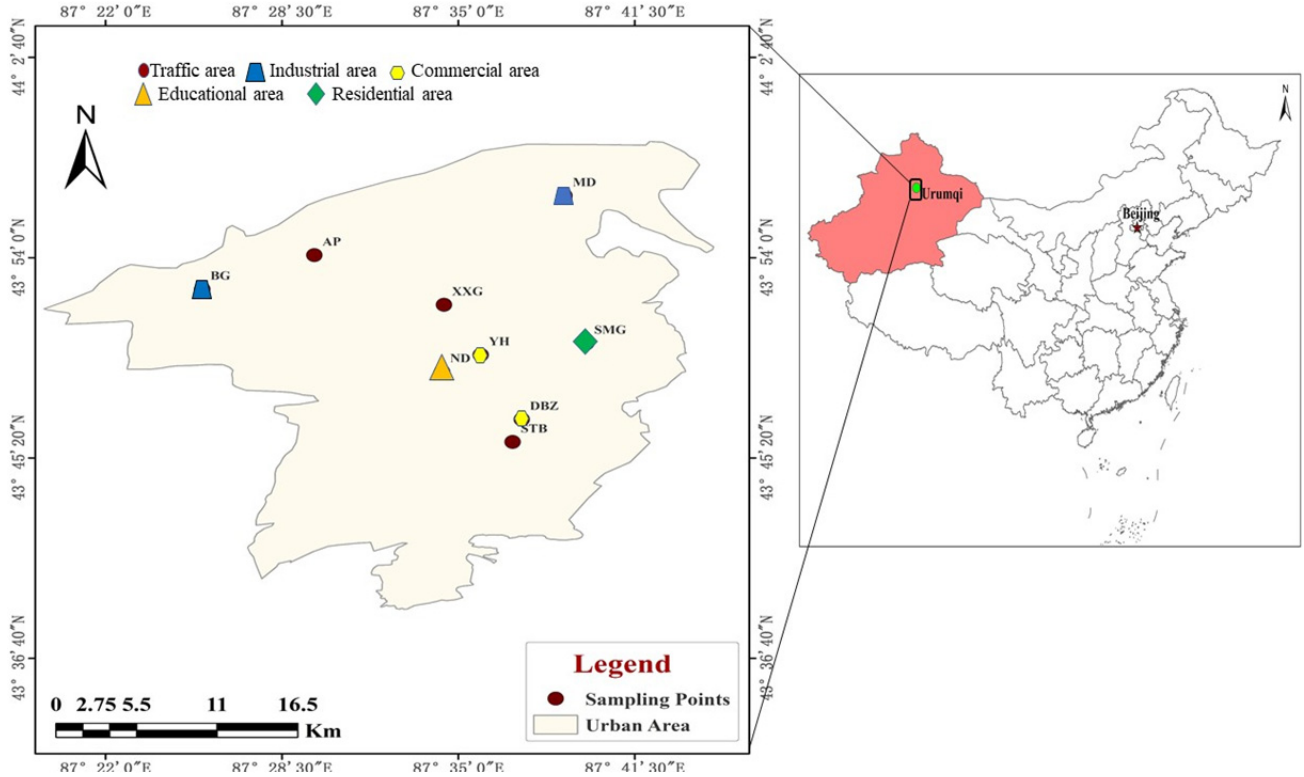

Fig. 1. Distribution map of sampling sites.

times and peak areas using a linear regression curve (Fig. S1) obtained from the standard solutions. The concentrations of 16 PAHs listed by the U.S. Environmental Protection Agency as priority PAHs were quantified according to their elution orders as followes: Naphthalene (Nap), Acenaphthylene (Acy), Fluorene (Flu), Acenaphthene (Ace), Phenanthrene (Phe), Anthracene (Ant), Fluoranthene (Flur), Pyrene (Pyr), Chrysene (Chry), Benzo[a]anthracene (BaA), Benzo[b]fluoranthene (BbF), Benzo[k]fluoranthene (BkF), Benzo[a]pyrene (BaP), Dibenzo[ah]anthracene (DbA), Benzo[ghi]perylene (BghiP), and Indeno[1,2,3-cd]pyrene (Ind).

In all analyses, for quality assurance and quality control, procedural (solvent) blanks and field blanks were performed periodically with the same procedure as the real samples, and no significant contamination was found. None of the target compounds were detected in the blank filters, indicating that the contamination of PAHs was negligible during transportation, storage, and analysis.

The average recovery efficiencies of the 16 PAHs in the standard mixture varied from 83.6% to 115.40%, and the relative standard deviations were between 1.9% and 15.03% with a mean value of 4.26%. The relative correlation coefficient of the standard curve determination (standard solution including six concentration grades: 0.1 μg mL^{-1}, 0.2 μg mL^{-1}, 0.5 μg mL^{-1}, 1.0 μg mL^{-1}, 2.0 μg mL^{-1}, 5.0 μg mL^{-1}) was higher than 0.99.

Health Risk Characterization

The BaP equivalent toxicity (BaP_{eq}) concentration has been widely used to assess the carcinogenic risk of a PAH mixture (Petry *et al.*, 1996; Tsai *et al.*, 2001). The BaP_{eq} in this study was calculated by multiplying the individual PAH concentrations in samples at each site during the two study periods with toxicity equivalency factors of target compounds (Petry *et al.*, 1996; Fang *et al.*, 2004b) with the equation:

$$\sum BaP_{eq} = \sum_{i}^{n=1} \left(C_i \times TEF_i \right) \quad (1)$$

where C_i and TEF_i are the concentration and toxic equivalent factors of i^{th} PAH congener. TEF_i values were taken from Fang *et al.* (2004b). The total carcinogenic potency of Σ_{16}PAHs for each period was estimated by summing the BaP_{eq} of all compounds.

The lifetime excess cancer risk (LCR) via inhalational exposure to PM-bound PAHs was also determined based on the resultant BaP_{eq} and WHO unit risk factor of BaP ($UR_{BaP} = 8.7 \times 10^{-5}$), which is 8.7 cases per 100,000 people with chronic inhalational exposure to 1 ng m^{-3} BaP over a lifetime of 70 years (WHO, 2000). The risk of developing lung cancer can thus be calculated as:

$$\mathrm{LCR} = \sum BaP_{eq} \times UR_{BaP} \quad (2)$$

RESULTS AND DISCUSSION

Temporal Variation of PAHs

Temporal Variation of PM and Σ_{16}PAHs

The average concentrations of PM_{10}, $PM_{2.5}$, and PAHs in

two particle size fractions obtained from each sampling site in Urumqi during heating and non-heating periods are presented in Fig. 2. Both PM and PAHs in PM exhibited a similar temporal variation among all sites observed in the two periods, resulting in high levels in the heating period and low levels in the non-heating period. Temporal variations have been widely reported for many studies, and the variability has been found to be dependent upon the unique climatic changes and anthropogenic activities of the sampling sites under investigation (Kong *et al.*, 2010; Teixeira *et al.*, 2012).

In the heating period, the average concentration of PM_{10} and $PM_{2.5}$ ranged from 192.60 to 276.23 μg m^{-3} and 132.60 to 206.47 μg m^{-3}, respectively, at nine sites. In the non-heating period, the concentration of both fractions dropped sharply compared to that in the heating period. PM_{10} concentrations in the non-heating period were 2.6–4.0-fold lower than those in the heating period, and $PM_{2.5}$ showed much bigger temporal variation (4.7–9.5 times) than PM_{10}. The average value of $PM_{2.5}/PM_{10}$ was 0.82 ± 0.16 in the heating period, which was two times higher than that in the non-heating period (0.40 ± 0.17).

The average concentrations of Σ_{16}PAHs in PM_{10} and $PM_{2.5}$ were 173.08 ng m^{-3} and 128.10 ng m^{-3} in the heating period and 60.85 ng m^{-3} and 49.03 ng m^{-3} in the non-heating period, respectively. The concentrations of the Σ_{16}PAHs in different sampling points varied significantly during the heating period. In contrast, the Σ_{16}PAHs concentrations were more consistent in the different sampling points in the non-heating period. As shown in Fig. 2, the concentrations of $PM_{2.5}$-bound Σ_{16}PAHs were slightly lower than the concentrations of PM_{10}-bound Σ_{16}PAHs. The results indicate that 80.8% of Σ_{16}PAHs distributed in particles with diameters less than 2.5 μm, and 19.2% of Σ_{16}PAHs distributed in particles with diameters of 2.5 to 10 μm ($PM_{2.5\text{-}10}$) during the heating period. During the non-heating period, the percentage of Σ_{16}PAHs in $PM_{2.5}$ was 74.0% and 26% in $PM_{2.5\text{-}10}$. As shown in Table 1, the results obtained in this work were compared with the total PAH concentrations observed in other parts of the country. Table 1 shows that the concentrations of PM-bound PAHs in this study are lower than in northern cities of China such as Beijing

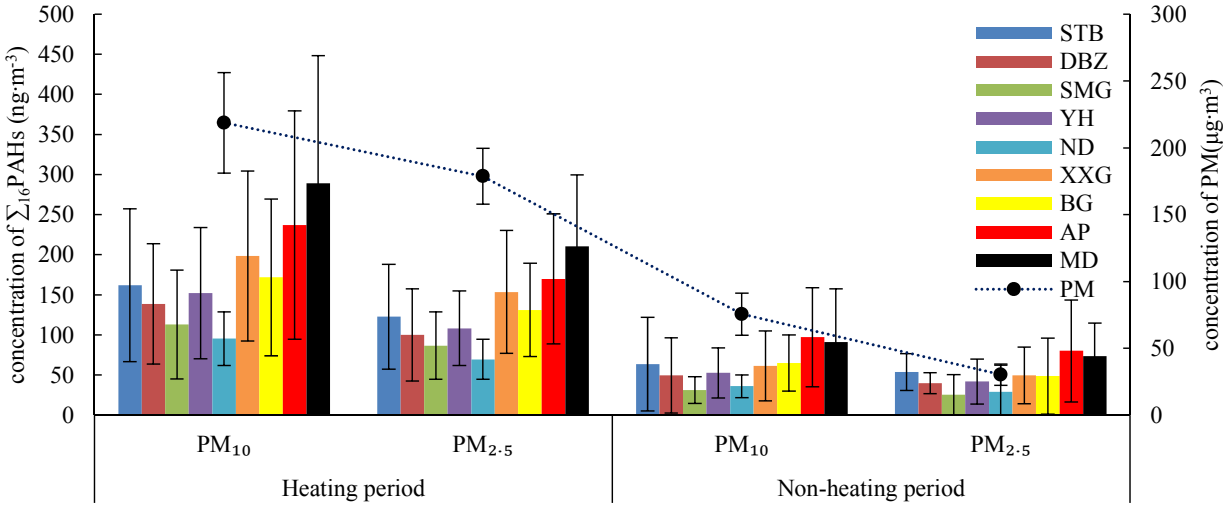

Fig. 2. Temporal variation of Σ_{16}PAHs.

Table 1. Comparisons with mean PM-bound PAHs derived from previous studies.

Cities	PM size	Total PAHs	PAHs Concentration (ng m^{-3})	Season	Reference
Urumqi	PM_{10}	Σ_{16}PAHs	173.08	Winter	In this study
	$PM_{2.5}$		128.10		
Urumqi	PM_{10}	Σ_{16}PAHs	60.85	Summer	In this study
	$PM_{2.5}$		49.3		
Shijiazhuang	$PM_{2.5}$	Σ_{16}PAHs	211.07	winter	Niu *et al.*, 2017
Beijing	$PM_{2.5}$	Σ_{16}PAHs	407.55	Winter	Wang *et al.*, 2008
	$PM_{2.5\text{-}10}$		244.04		
Xi'an	PM_{10}	Σ_{15}PAHs	344.2 ± 149.7	Winter	Okuda *et al.*, 2010
			136.7 ± 56.7	Summer	
Nanjing	$PM_{2.5}$	Σ_{18}PAHs	3.77–15.59	Summer	Li *et al.*, 2016
E'erduosi	$PM_{2.5}$	Σ_{18}PAHs	0.58–145.01	Summer	Wu *et al.*, 2014
	PM_{10}		5.80–180.32		
Urumqi	PM_9	Σ_{14}PAHs	216 ± 112	Winter	Ren *et al.*, 2017
Guangzhou	$PM_{2.5}$	Σ_{17}PAHs	45.52	Winter	Liu *et al.*, 2015
			10.43	Summer	

(Wang *et al.*, 2008), Tianjin (Niu *et al.*, 2017) and Xi'an (Okuda *et al.*, 2010) but are higher than southern cities such as Nanjing (Li *et al.*, 2016) and Guangzhou (Liu *et al.*, 2015).

As presented in Fig. 2, significant temporal variations were observed in all sites, with higher levels of Σ_{16}PAHs in the heating period than in the non-heating period. During the non-heating period, the Σ_{16}PAHs concentrations in both fractions were much lower than those in the heating period. Similar temporal trends have been reported in four other Asian megacities, namely, Beijing, Kolkata, Hanoi, and Tokyo (Saha *et al.*, 2017). The main reasons that the higher PAHs occur in winter are (a) increased emissions from heating systems during the 6-month long heating period in Urumqi; (b) the cold starting conditions of vehicles in winter may also contribute to the increase in PAH concentration (Ravindra *et al.*, 2006; Kong *et al.*, 2010); and (c) low atmospheric temperature enhances sorption of the most volatile PAHs on particles, and typical meteorological conditions in winter were favorable for the gathering of atmospheric PAHs in particles (Kiss *et al.*, 2001). Importantly, an inversion layer frequently occurs in Urumqi during the heating period, which is not conducive to the diffusion of pollutants. Lower PAH levels in summer were likely attributed to the combined effect of the quick atmospheric dispersion of pollutants, the wash-out effect of rain, the increase in photodegradation and a higher percentage in the vapor phase (Guo *et al.*, 2003).

Temporal Variation of Individual PAHs and Ring Distribution

The examined PAHs can be classified according to their number of aromatic rings as follows: 2-ring, including Nap; 3-ring, including Acy, Flu, Ace, Phe and Ant; 4-ring, including Flur, Pyr and Chry; 5-ring, including BaA, BbF, BkF and BaP; and 6-ring, including DbA, BghiP and Ind. According to the molecular weight, the PAHs can be further divided into low molecular weight (LMW, 2- and 3-ring) PAHs, middle molecular weight (MMW, 4-ring) PAHs and high molecular weight (HMW, 5- and 6-ring) PAHs.

The temporal variation of individual PAHs in PM_{10} and $PM_{2.5}$ are presented in Fig. 3. MMW PAHs have a higher contribution, and Pyr is the most abundant PAH congener in the heating period, followed by BbF, Chry, BaA, and Flur. In the non-heating period, HMW PAHs, including BbF, BkF, BaP, BghiP, DbA, and InP, accounted for 56% of the Σ_{16}PAHs. LMW PAHs, such as NAP, Acy and Flu, exhibited higher contributions in the heating period than in the non-heating period, and Ant was not detected in the non-heating period samples, owing to their volatility. BghiP, InP, BkF, BbF and Chry compounds are indictors of vehicular emissions, while the compounds of Pyr, Flur, BbF, and Ant are abundant in coal combustion emission (Khalili *et al.*, 1995; Kong *et al.*, 2010). Flur, Chry, and BaA are associated with natural gas combustion, and BaA is a tracer component (Bourotte *et al.*, 2005). Variation of individual PAHs in different periods revealed that the emission types of PAHs during the heating period are different than those in the non-heating period.

Ring compositional patterns of Σ_{16}PAHs were not consistent in different periods (Fig. 4). During the heating period, 4-ring PAHs occupied 41% of Σ_{16}PAHs, followed by 5-ring (32%), 2- and 3-ring (14%), and 6-ring (13%). In the non-heating period, the percentage of LMW PAHs and MLW PAHs was lower than those in the heating period by 4% and 5%, respectively. The proportion of the HMW PAHs increased by 11% during the non-heating period. Bari *et al.* (2010) also reported that HMW PAHs are dominant in the particle phase in Europe.

The compositional patterns of Σ_{16}PAHs in the PM_{10} and $PM_{2.5}$ samples were similar, and over 85% of the detected PAHs had 4–6 aromatic rings. PAHs with different ring numbers originate from different emission sources. 5- and 6-ring PAHs, such as Pyr, BaP, Inp and BghiP, are characteristic compounds of traffic pollution, and 4-ring PAHs, such as Flur, Pyr and Chry, are characteristic compounds of coal combustion and natural gas combustion (Bourotte *et al.*, 2005; Wang *et al.*, 2009). In the current work, the percentages

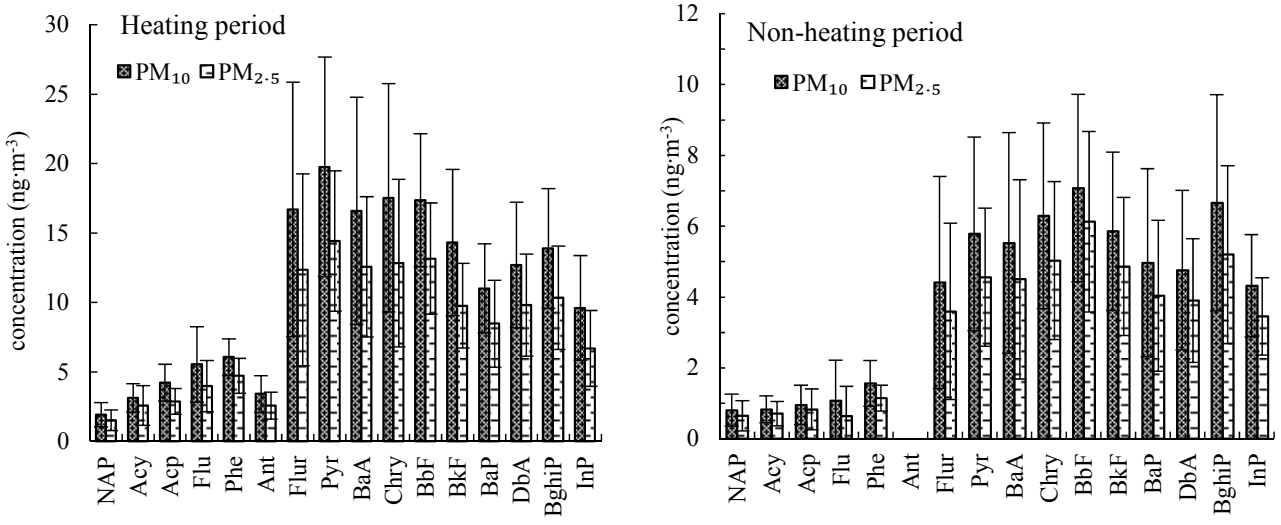

Fig. 3. Temporal variation of individual PAHs.

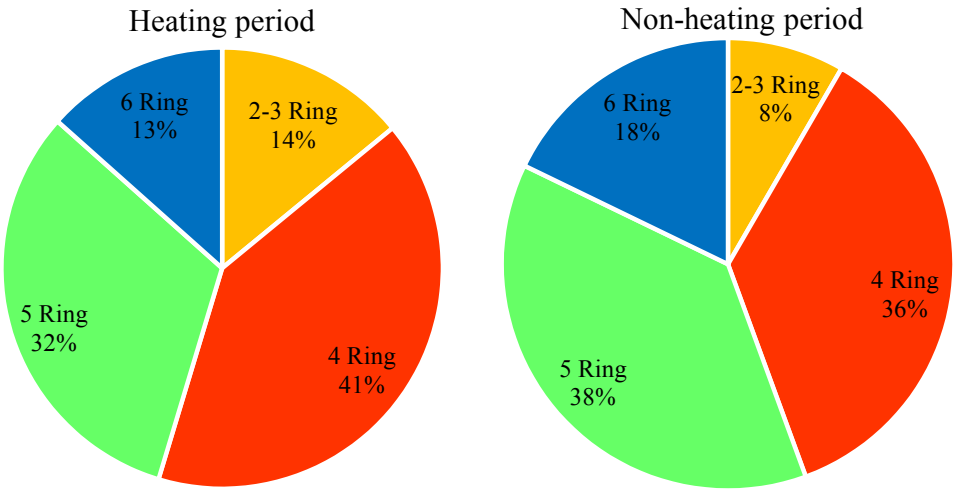

Fig. 4. Ring distribution of PAHs.

of 4-ring PAHs decreased by 5% in the non-heating period because of their semi-volatile characteristics, which were more highly distributed in the gas phase in the hot season than in other seasons. In contrast, the percentages of 5- and 6-ring PAHs in the non-heating period increased more than in the heating period, reflecting the source variation of PAHs in the two periods.

Spatial Distribution of PAHs

Although more work has been done on comparing atmospheric PAHs in urban and suburban areas (Zhou *et al.*, 2005; Moon *et al.*, 2006), few studies have been conducted on the comparison of PAHs in different functional zones (Gao *et al.*, 2016). To investigate the spatial variation of PAHs in Urumqi, this research was performed in five functional areas and at nine sampling sites. Concentrations, distribution patterns and profiles of PAHs at all sites are summarized in Figs. 2 and 5. Owing to the differences in geographical position, traffic density, and industry distribution, the contribution of pollutants from anthropogenic inputs varied in different functional zones.

The complicated topography and geomorphology of Urumqi have caused extreme differences in the spatial distribution of pollutant concentrations (Wu *et al.*, 2008). Generally, the sites located in northern parts of the city have higher PAH concentrations than those located in southern parts during both periods (Fig. 5). This result could be due to the peculiar characteristics of the northern site, including multi-pollutant sources such as heavy-duty vehicle exhaust and industrial emissions; the effects of local anthropogenic emissions and long-distance transport from neighboring cities may also be important.

In the heating period, the site MD, where most of the heavily contaminated enterprises were located, had the highest levels of PAHs in PM_{10} and $PM_{2.5}$, with average concentrations of 289.76 ng m^{-3} and 210.77 ng m^{-3}, respectively. At the MD site, 4-ring PAHs, which are characteristic of coal combustion, were the most abundant components in this area (Fig. 6). In addition to the industrial area, traffic area sites, such as AP, XXG, and STB, also had large amounts of PAHs, and characteristic vehicle-emitted 5- and 6-ring PAHs, such as BghiP, InP, and BbF, were the most common compounds of Σ_{16}PAHs. Site ND (educational area) was relatively clean, with mean values of 95.33 ng m^{-3} and 69.66 ng m^{-3} for PM_{10} and $PM_{2.5}$, respectively, which were both 3 times lower than those in the industrial site. The concentrations of Σ_{16}PAHs at different sites follow the following order: MD (289.76 ng m^{-3}, 210.77 ng m^{-3}) > AP (236.92 ng m^{-3}, 169.88 ng m^{-3}) > XXG (198.46 ng m^{-3}, 153.70 ng m^{-3}) > BG (171.86 ng m^{-3}, 131.15 ng m^{-3}) > STB (162.14 ng m^{-3}, 122.85 ng m^{-3}) > YH (152.06 ng m^{-3}, 108.30 ng m^{-3}) > DBZ (138.58 ng m^{-3}, 51.48 ng m^{-3}) > SMG (113.18 ng m^{-3}, 86.74 ng m^{-3}) > ND (95.38 ng m^{-3}, 69.66 ng m^{-3}). According to the functional area, the concentrations of Σ_{16}PAHs were in the following order: industrial area > traffic area > commercial area > residential area > educational area, showing similar spatial distribution trends with Beijing (Gao *et al.*, 2016).

In the non-heating period, the content of particulate PAHs dramatically decreased at all sites. PAH levels at the airport (AP) site exceeded the industrial area of the MD site. These higher levels at the airport may be explained by higher PAH emissions from vehicles and airplanes, as well as non-local pollutants transported from the surrounding areas. As seen in Fig. 6, 2- to 4-ring PAHs are main components of Σ_{16}PAHs in the industrial area because of coal combustion; under warm conditions, these PAHs tend to partition from the particle phase towards the gas phase due to their semi-volatile properties (Teixeira *et al.*, 2012). In contrast, 5- and 6-ring PAHs are common compounds in traffic areas, are mainly absorbed in particles (Wu *et al.*, 2014), and may cause the higher concentration of particulate PAHs in traffic areas. The lowest value of PAHs detected at the SMG and ND sites resulted from the reduction of emission sources for these two points during the non-heating period. The order of Σ_{16}PAHs at the different sites was as follows: AP (97.27 ng m^{-3}, 80.03 ng m^{-3}) > MD (90.81 ng m^{-3}, 73.27 ng m^{-3}) > BG (65.07 ng m^{-3}, 48.59 ng m^{-3}) > STB (63.61 ng m^{-3}, 53.79 ng m^{-3}) > XXG (61.44 ng m^{-3}, 49.62 ng m^{-3}) > YH (52.74 ng m^{-3}, 41.82 ng m^{-3}) > DBZ (49.48 ng m^{-3},

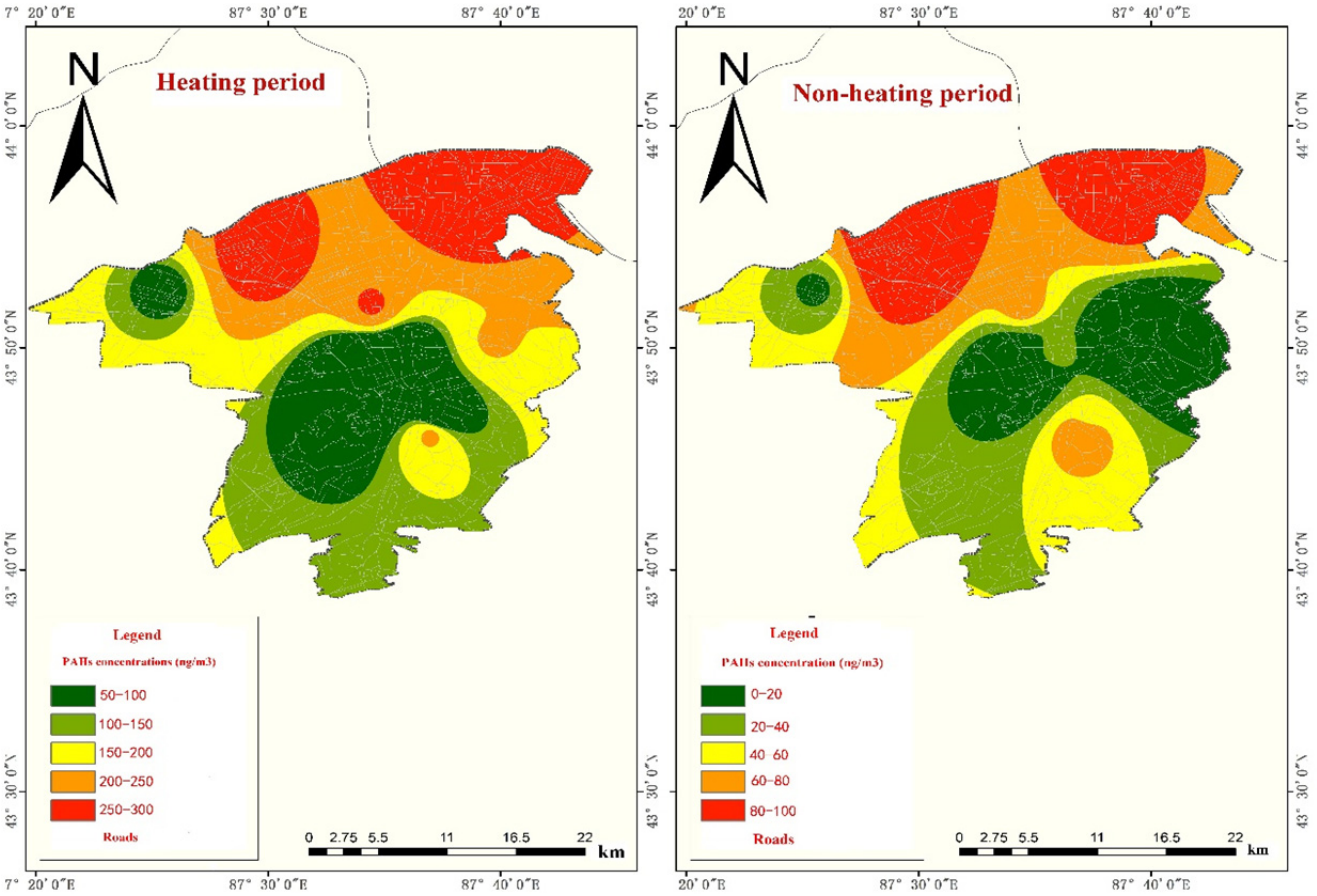

Fig. 5. Spatial distribution of Σ_{16}PAHs during two periods.

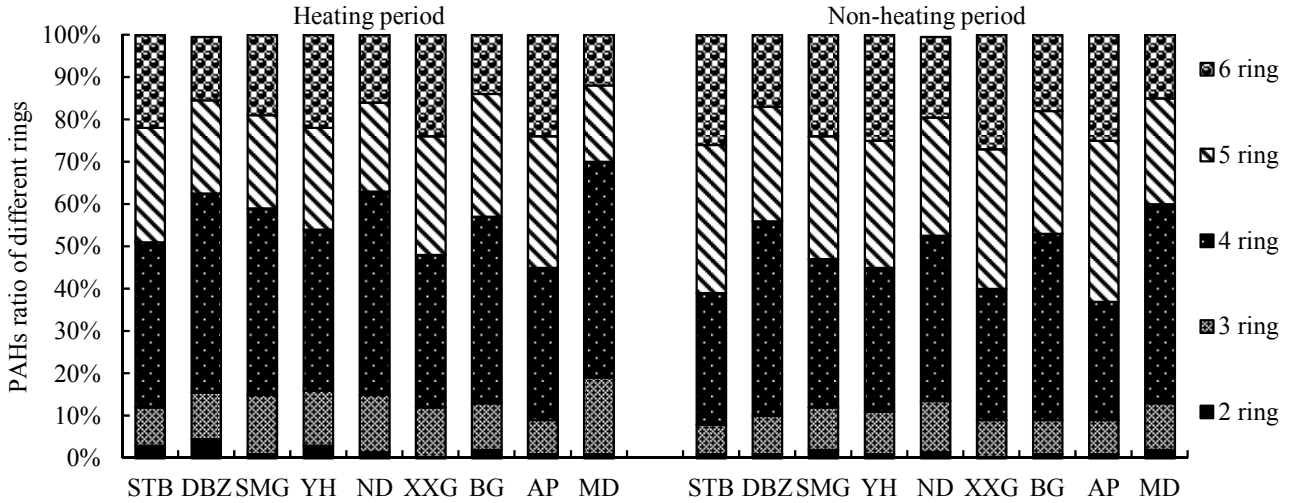

Fig. 6. Temporal variation of PAHs compounds at different sampling sites.

39.75 ng m^{-3}) > ND (35.97 ng m^{-3}, 28.95 ng m^{-3}) > SMG (31.26 ng m^{-3}, 25.42 ng m^{-3}). The order at different functional areas was as follows: traffic area > industrial area > commercial area > educational area > residential area.

Source Analysis of PAHs

Diagnostic Ratio Analysis

The composition of PAHs produced by different combustion processes is different due to the diversity of fuels and combustion conditions (Maioli *et al.*, 2010). LMW PAHs are usually formed by low-temperature processes such as wood and coal burning, whereas high-temperature processes (e.g., fuel combustion in engines) produce HMW PAHs (Tobiszewski and Namieśnik, 2012). PAH diagnostic ratios have been used to distinguish diesel/gasoline combustion emissions (Ravindra *et al.*, 2008), biomass

burning processes, and coal combustion processes (Yunker *et al.*, 2002). In our study, the characteristic ratios of PAHs in PM_{10} and $PM_{2.5}$ were essentially similar. Wang *et al.* (2006) confirmed that diagnostic ratios do not change with particle size. Therefore, the values of individual PAHs in $PM_{2.5}$ were used for diagnostic ratios. The concentration ratios of combustion PAHs (Flur + Pyr + BaA + Chry + BbF + BkF + BaP + BghiP + InP) to the total PAHs (CPAHs/Σ_{16}PAH) of 0.87, 0.78 and 0.73 indicate the biomass/coal combustion sources, diesel engine emissions, and gasoline engine emissions, respectively (Mantis *et al.*, 2005; Shi *et al.*, 2010). Ratios of Flur/(Flur + Pyr) > 0.5, BaP/BghiP < 0.6, and 0.2 < BaA / (BaA + Chr) < 0.35 indicate biomass/coal combustion, while the ratios of Flur/(Flur + Pyr) < 0.5, BaP/BghiP > 0.6, and 0.35 < BaA/(BaA + Chr) < 0.64 indicate traffic emissions (Yunker *et al.*, 2002; Katsoyiannis *et al.*, 2007; Park *et al.*, 2011). Molecular diagnostic ratios for the present work are presented in Fig. 7 and Table S3.

According to the ratios of Flur/(Flur + Pyr), BaP/BghiP, BaA/(BaA + Chr), and CPAHs/Σ_{16}PAH, in total, the particulate PAHs at all nine sites mainly originated from combustion sources with a variable seasonal contribution.

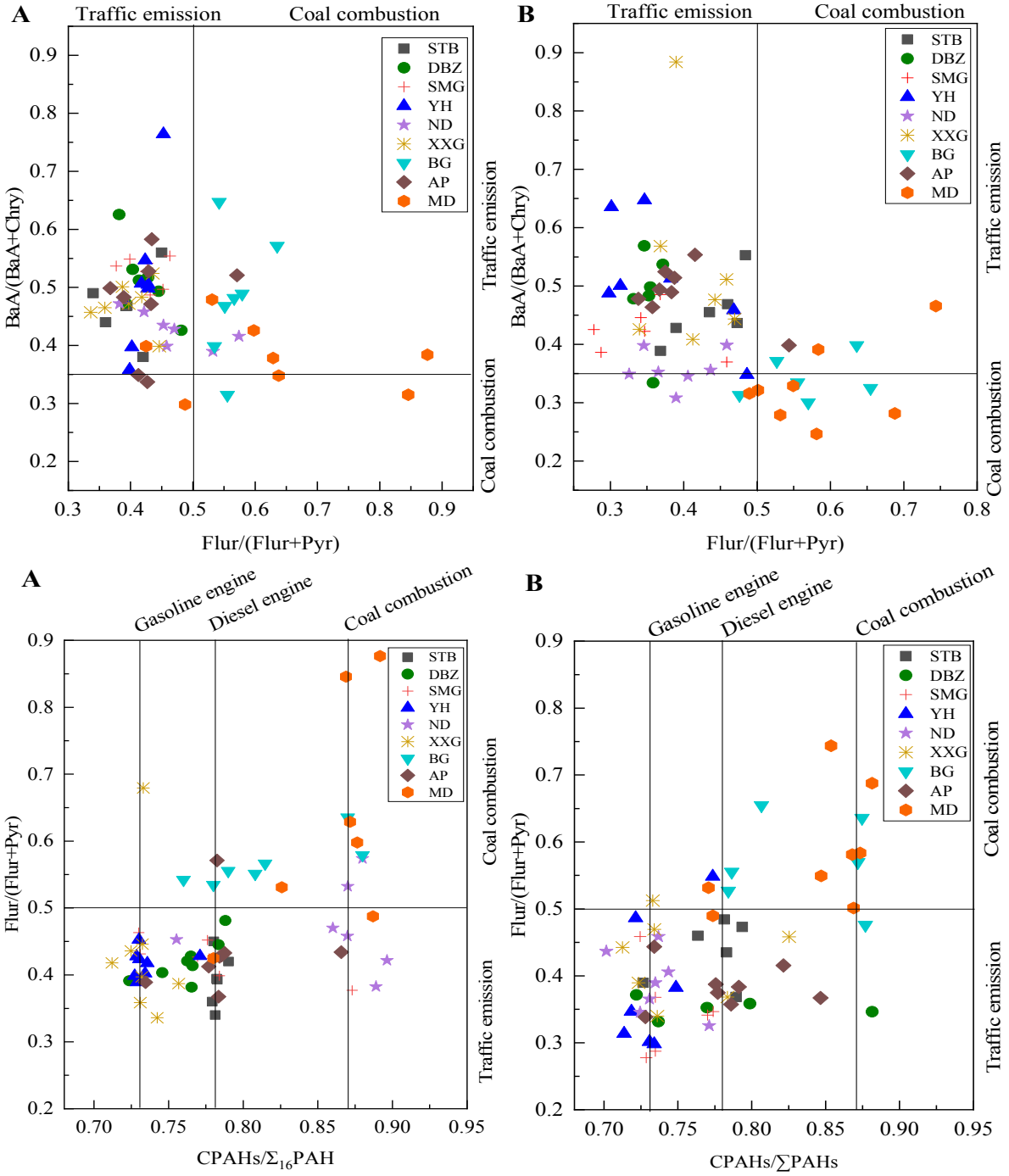

Fig. 7. Graphic illustration of the diagnostic ratios for the sources of PAHs. A: Heating period; B: Non-heating period.

As summarized in Fig. 7, the ratios of CPAHs/ Σ_{16}PAH were higher in the heating period than those in the non-heating period at almost all sites. This results indicates that biomass/coal combustion makes considerable contributions in the heating period, and these results are consistent with those previously reported in other areas (Mantis *et al.*, 2005; Shi *et al.*, 2010). Moreover, the scatter plot of Flur/(Flur + Pyr) and CPAHs/Σ_{16}PAH confirmed that the PAHs at the industrial sites (MD and BG) originated from a combination of diesel engine emissions and biomass/coal combustion. This finding seems reasonable to a certain extent, as various industrial activities and heavy-duty trucks may affect this area. The ratios of CPAHs/Σ_{16}PAH and BaP/BghiP indicated that gasoline and diesel emissions were the largest contributor to transportation sectors such as the AP, XXG, YH and STB sites. Furthermore, the traffic sites (XXG and YH) downtown were dominated by gasoline engine emissions, while diesel engine emissions dominated at the AP and STB sites. At the AP site, however, characteristic biomass and coal combustion PAHs were detected in both periods. The results are also supported by the ratio of BaP/(BaP + Cry) (Fang *et al.*, 2004a) and InP/(InP + BghiP) (Ravindra *et al.*, 2008), which presented a combination of several sources. At residential, educational, and commercial sites, the diagnostic ratios showed a significant contribution of vehicle exhaust, with relatively lower contributions from biomass/coal combustion.

Principle Component Analysis (PCA)

In addition to using diagnostic ratios, a PCA was undertaken to further identify the major sources of PAH emissions in Urumqi. The PCA results indicate the factors that can explain the main data variance; therefore, individual PAHs representative of each factor were chosen as source tracers (Fang *et al.*, 2004a). In this study, a PCA was conducted on the PAH datasets of $PM_{2.5}$ in both periods.

During the heating period, the four principal components, PC1, PC2, PC3, and PC4, explained 36.51%, 33.10%, 13.54%, and 10.58% (93.73% total) of the total variance of data, respectively (Table 2). PC1 explained 36.51% of the data variance, with loadings of DbA, BbF, BkF, InP, BghiP, and Phe, which are PAH congeners indicative of vehicular emissions. According to previous studies, the compounds DbA, InP, and BghiP are characteristic of gasoline emissions, while BbF, BkF, and Phe are the predominant PAH species in diesel emissions (Khalili *et al.*, 1995; Kong *et al.*, 2010). Therefore, PC1 was selected to represent vehicular emissions (a mixture of gasoline and diesel emissions). PC2 (33.10% of the total variance) was highly loaded with LMW and MMW PAHs, such as NAP, BaA, Chry, Pry, Flur, and BaP, and moderately loaded with InP and BkF. BaA and Chry were found to be predominant compounds of natural gas combustion, and BaA is tracer species (Kavouras *et al.*, 2001; Bourotte *et al.*, 2005). In contrast, Khalili *et al.* (1995) and Kong *et al.* (2010) reported that Flur, NAP, Pyr, Phe, Chry, and BaA also indicated coal combustion sources. Thus, PC2 is regarded as coal and natural gas combustion. PC3 and PC4 contributed 13.54% (Flu and Ant) and 10.58% (Acp and Acy) to the total variance, respectively. According to Khalili *et al.* (1995), Flu and Ant are major sources of biomass combustion. Accordingly, in this work, PC3 was selected for biomass burning. Experimental studies by Simcik *et al.* (1999) have shown that Acp and Acy can be regarded as petrochemical or steel industry sources, using heavy oils as fuel. As a result, PC4 was chosen for stationary industrial sources and coke ovens.

In the non-heating period, three components (81.20%) were identified by PCA, and the results were more complicated than those in the heating period. PC1 accounted for

Table 2. Factor loadings of PCA for both heating and non-heating periods.

PAHs	Heating period				Non-heating period		
	PC1	PC2	PC3	PC4	PC1	PC2	PC3
DbA	0.890				0.901		
BbF	0.839				0.937	0.626	
BghiP	0.822				0.745		
Phe	0.803					0.559	
Pyr	0.543	0.707			0.962		
InP	0.756	0.658			0.672		
BkF	0.710	0.628				0.921	
Flur		0.880			0.892		
NAP		0.858					0.658
BaP		0.793			0.910		
BaA		0.792			0.936		
Chry		0.787			0.922		
Flu			0.844			0.652	
Ant			0.905				
Acp				0.822			0.667
Acy				0.928			0.708
Variance (%)	36.51	33.10	13.54	10.58	46.20	21.00	14.00

Extraction Method: Principal Component Analysis; Rotation Method: Varimax with Kaiser Normalization; Factor loading ≥ 0.5 listed.

46.20% of the variance, with high loadings of DbA, BbF, BghiP, Pyr, Flur, InP, BaP, BaA, and Chry, which are the MMW and HMW PAHs. PC1 seemed to be within the scope of vehicular emissions (BbF, BghiP, and InP), coal combustion (Pyr, BaP, Flur, and Chry) and natural gas combustion (BaA and Chry) sources (Simcik *et al.*, 1999; Kavouras *et al.*, 2001). This finding indicates that PC1 can be regarded as mixing sources of coal/natural gas combustion and vehicular emissions. PC2 (21.00%) could be attributed to diesel vehicular emissions with high loadings of BkF, Flu, and Phe and moderate loadings of BbF. PC3 (14.00%) showed a pattern of stationary industrial sources and coke ovens and was similar to PC4 in the heating period.

In conclusion, the combination of PCA and diagnostic ratios revealed that vehicle exhaust was the major source of PAHs for both the heating and non-heating periods at central urban sites and traffic sites, while heavy-duty vehicular emissions and biomass/coal combustion emissions existed simultaneously in the industrial area. It should be noted that the diagnostic ratios and PCA model could not distinguish regional transport from local emissions. However, the impacts of PAHs drifting from the surrounding cities of Urumqi cannot be neglected.

Toxicity and Carcinogenic Risk Assessment of PAHs

BaP is considered one of the most toxic PAHs and is the only PAH that has national standards. During the non-heating period, the average concentration of BaP in PM_{10} was 3.07 ng m^{-3}, which was higher than the National Standard GB3095-2012 for the 24 h average concentration of 2.5 ng m^{-3} and the annual average concentration standard of 1.0 ng m^{-3}. In $PM_{2.5}$, the average concentration of BaP was 1.96 ng m^{-3} and was higher than the annual standard but lower than the daily standard. However, BaP concentrations in the heating period in both fractions were approximately 2-fold higher than those in the non-heating period, indicating a greater risk to human health.

As seen in Fig. 8, the calculated ΣBaP_{eq} levels in the heating period were higher than those in the non-heating period. In addition, the ΣBaP_{eq} at different sites ranged from 17.6 to 37.9 ng m^{-3} and from 4.4 to 19.5 ng m^{-3} during heating and non-heating periods, respectively, and were the maximum values, observed at the airport, followed by the industrial area for the MD site for both periods. Generally, the sites in the northern part of the city including MD, AP, BG, and XXG accounted for approximately 60% of ΣBaP_{eq}. In the non-heating period, fluctuations of ΣBaP_{eq} at different sites were not as significant as those in the heating period, and the four sites including STB, DBZ, YH, and BG showed a similar contribution to ΣBaP_{eq}, with mean values of 10.25%, 10.25%, 10.57%, and 10.23%, respectively. In fact, people living in the industrial and traffic areas may have a greater inhalation cancer risk than people residing in the living and educational areas. However, ΣBaP_{eq} values were higher than those reported in Guangzhou (0.96–22.46 ng m^{-3}) and were comparable to the range of ΣBaP_{eq} of 2–64 ng m^{-3} (average: 17 ng m^{-3}) in Xi'an (Bandowe *et al.*, 2014; Liu *et al.*, 2015).

As mentioned previously, PAHs from vehicular exhaust, including Chr, BaA, BaP, DbA, BbF, and InP, may be considered potential human carcinogens (Teixeira *et al.*, 2012). Based on the BaP_{eq} calculation, BaP and DbA contributed to more than 80% of the carcinogenicity of the PAHs in the samples, on average, because of their high toxicity equivalency factors, followed by BbF, BkF, and InP. These findings confirm the importance of BaP and DbA as surrogate compounds in assessing PAH risks in the Urumqi atmosphere. On average, DbA contributed more than Bap during the heating period, and the opposite result was displayed in the non-heating period (Fig. 8). A similar contribution of BaP and DbA to carcinogenic activity is reported in previous studies (Amador-Muñoz *et al.*, 2010).

As shown in Fig. 8, the average LCR decreased from 1.4×10^{-4} (range: 9.6×10^{-5}–2.1×10^{-4}) in the heating period to 6.0×10^{-5} (range: 2.4×10^{-5}–1.1×10^{-4}) in the non-heating period. This result indicates that average of 140 (range: 96–210) in the heating period and 60 (range: 24–110) in the non-heating period cancer cases per million residents

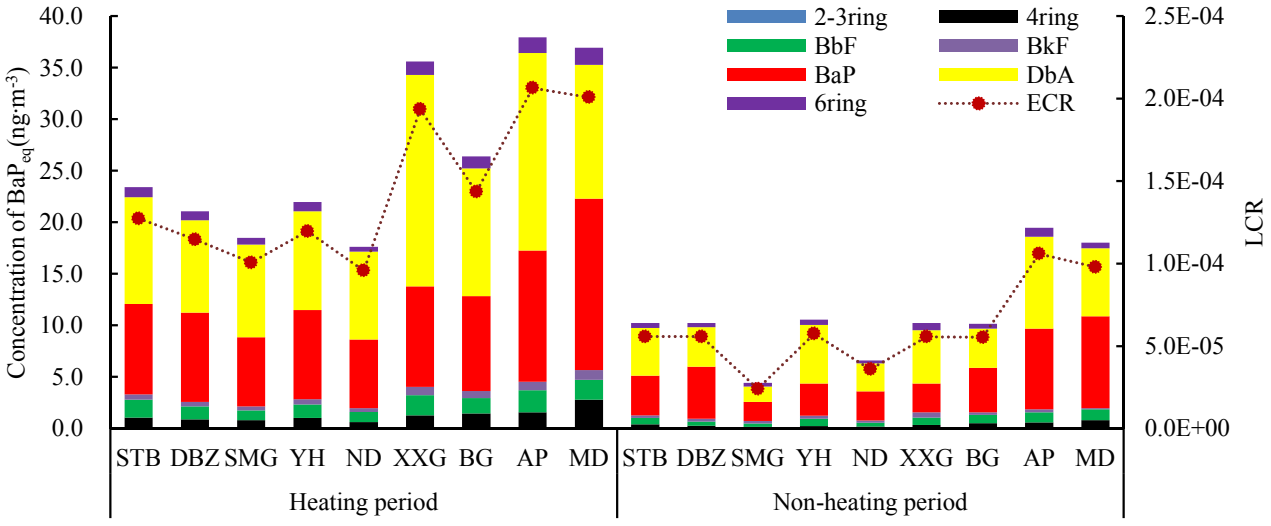

Fig. 8. spatiotemporal variation of BaP_{eq} and LCR.

in Urumqi could be attributable to the inhalation of PM-bound PAHs. The cancer cases calculated with similar methods for Guangzhou (598; range: 84–1950) and Xi'an (1450; range: 140–5600) were higher than those in this study, while the values for this study were higher than those estimated for Nanjing (5.1 cases per million) and Zaragoza, Spain (82 cases per million) (Bandowe *et al.*, 2014; Callén *et al.*, 2014; Liu *et al.*, 2015; Li *et al.*, 2016).

In conclusion, these results highlight a profound cancer risk for human health due to high pollution levels in the atmosphere. On the bases of these sources, the results indicated the importance of controlling emissions from vehicle exhaust as well as industrial activity to mitigate the potential risk from exposure to high-level carcinogenic PAHs.

Uncertainty Analysis

There were unavoidable uncertainties during the evaluation process. First, due to the volatility of LMW PAHs, we could not measure the concentrations of some of the 2- and 3-ring PAHs in our non-heating samples. Second, we could not separate the contribution of local sources and long-distance transportation from the adjacent city group using the diagnostic ratios and PCA, as PAH source profiles are not unique by source type. Third, the LCR estimation is based on the population exposure level of PM through generalizing individual differences, which could also induce the uncertainty of the health risks in this study.

CONCLUSION

The results of the current study show the obvious spatiotemporal variation in the PAH concentrations and ring compositional patterns in Urumqi. Higher PAH concentrations characterized by 4-ring PAHs were detected during the heating period. The northern parts of the city (the MD, BG, and AP sites) represented the most polluted areas of Urumqi due to natural gas/biomass/coal combustion and a large number of heavy-duty vehicular emissions. The source apportionment results for the PAHs show considerable differences between the sources of PM-bound PAHs during the heating and non-heating periods. Vehicular traffic emissions were the primary source of PM-bound PAHs in the central urban area, while natural gas/biomass/coal combustion was the main source in the industrial area. The results from evaluating the BaP equivalent toxicity (BaP_{eq}) indicate that BaP and DbA were the most toxic components, with the largest impact on human health, among the 16 PAHs. The calculation of the LCR suggests that the number of cancer risk cases related to PAH exposure decreased from 140 persons per million residents in Urumqi during the heating period to 60 persons during the non-heating period.

ACKNOWLEDGMENTS

I would like to thank Professor Shaodong Xie and his research team for the useful comments and suggestions. This work was financially supported by the Natural Science Foundation Key Project (No. 21167017) and (No. 21567028).

SUPPLEMENTARY MATERIAL

Supplementary data associated with this article can be found in the online version at http://www.aaqr.org.

REFERENCES

Amador-Muñoz, O., Villalobos-Pietrini, R., Agapito-Nadales, M.C., MuniveColin, Z., Hernandez-Mena, L., Sanchez-Sandoval, M., Gomez-Arroyo, S., Bravo-Cabrera, J.L. and Guzman-Rincon, J. (2010). Solvent extracted organic matter and polycyclic aromatic hydrocarbons distributed in size-segregated airborne particles in a zone of México City: Seasonal behavior and human exposure. *Atmos. Environ*. 44: 122–130.

Apte, J.S., Marshall, J.D., Cohen, A.J. and Brauer, M. (2015). Addressing global mortality from ambient $PM_{2.5}$. *Environ. Sci. Technol.* 49: 8057–8066.

Bandowe, B.A., Meusel, H., Huang, R. J., Ho, K., Cao, J., Hoffmann, T. and Wilcke, W. (2014). $PM_{2.5}$-bound oxygenated PAHs, nitro-PAHs and parent-PAHs from the atmosphere of a Chinese megacity: Seasonal variation, sources and cancer risk assessment. *Sci. Total Environ*. 473–474: 77–87.

Bari, M.A., Baumbach, G., Kuch, B. and Scheffknecht, G. (2010). Particle-phase concentrations of polycyclic aromatic hydrocarbons in ambient air of rural residential areas in southern Germany. *Air Qual. Atmos. Health* 3: 103–116.

Bourotte, C., Forti, M.C., Taniguchi, S., Bícego, M.C. and Lotufo, P.A. (2005). A wintertime study of PAHs in fine and coarse aerosols in São Paulo city, Brazil. *Atmos. Environ*. 39: 3799–3811.

Callén, M. S., Iturmendi, A. and López, J. M. (2014). Source apportionment of atmospheric $PM_{2.5}$-bound polycyclic aromatic hydrocarbons by a PMF receptor model. Assessment of potential risk for human health. *Environ. Pollut*. 195: 167–177.

Chou, W.C., Hsu, C.Y., Ho, C.C., Hsieh, J.H., Chiang, H.C., Tsou, T.C., Chen, Y.C. and Lin, P. (2017). Development of an in vitro-based risk assessment framework for predicting ambient particulate matter-bound polycyclic aromatic hydrocarbon-activated toxicity pathways. *Environ. Sci. Technol.* 51: 14262–14272.

Fang, G. C., Chang, K. F., Lu, C. and Bai, H. (2004b). Estimation of PAHs dry deposition and bap toxic equivalency factors (TEFs) study at urban, industry park and rural sampling sites in central Taiwan, Taichung. *Chemosphere* 55: 787–796.

Fang, G.C., Chang, C.N., Wu, Y.S., Fu, P.P., Yang, I.L. and Chen, M.H. (2004a). Characterization, identification of ambient air and road dust polycyclic aromatic hydrocarbons in central Taiwan, Taichung. *Sci. Total Environ.* 327: 135–146.

Fu, X., Cheng, Z., Wang, S., Hua, Y., Xing, J. and Hao, J. (2016). Local and regional contributions to fine particle pollution in winter of the Yangtze River Delta, China. *Aerosol Air Qual. Res.* 16: 1067–1080.

Gao, Y., Guo, X., Ji, H., Li, C., Ding, H., Briki, M., Tang,

L. and Zhang, Y. (2016). Potential threat of heavy metals and PAHs in $PM_{2.5}$ in different urban functional areas of Beijing. *Atmos. Res*. 178–179: 6–16.

Guo, H., Lee, S.C., Ho, K.F., Wang, X.M. and Zou, S.C. (2003). Particle-associated polycyclic aromatic hydrocarbons in urban air of Hong Kong. *Atmos. Environ.* 37: 5307–5317.

He, J., Fan, S., Meng, Q., Sun, Y., Zhang, J. and Zu, F. (2014). Polycyclic aromatic hydrocarbons (PAHs) associated with fine particulate matters in Nanjing, China: Distributions, sources and meteorological influences. *Atmos. Environ.* 89: 207–215.

Katsoyiannis, A., Terzi, E. and Cai, Q.Y. (2007). On the use of PAH molecular diagnostic ratios in sewage sludge for the understanding of the PAH sources. Is this use appropriate? *Chemosphere* 69: 1337–1339.

Kavouras, I.G., Koutrakis, P., Tsapakis, M., Lagoudaki, E., Stephanou, E.G., Von, B.D. and Oyola, P. (2001). Source apportionment of urban particulate aliphatic and polynuclear aromatic hydrocarbons (PAHs) using multivariate methods. *Environ. Sci. Technol.* 35: 2288–2294.

Khalili, N.R., Scheff, P.A. and Holsen, T.M. (1995). PAH source fingerprints for coke ovens, diesel and, gasoline engines, highway tunnels, and wood combustion emissions. *Atmos. Environ*. 29: 533–542.

Kiss, G., Varga-Puchony, Z., Tolnai, B., Varga, B., Gelencsér, A., Krivácsy, Z. and Hlavay, J. (2001). The seasonal changes in the concentration of polycyclic aromatic hydrocarbons in precipitation and aerosol near Lake Balaton, Hungary. *Environ. Pollut*. 114: 55–61.

Kong, S., Ding, X., Bai, Z., Han, B., Chen, L., Shi, J. and Li, Z. (2010). A seasonal study of polycyclic aromatic hydrocarbons in $PM_{2.5}$ and $PM_{2.5\text{-}10}$ in five typical cities of Liaoning Province, China. *J. Hazard. Mater.* 183: 70–80.

Kong, S., Ji, Y., Li, Z., Lu, B. and Bai, Z. (2013). Emission and profile characteristic of polycyclic aromatic hydrocarbons in $PM_{2.5}$ and PM_{10} from stationary sources based on dilution sampling. *Atmos. Environ*. 77: 155–165.

Li, X., Kong, S., Yin, Y., Li, L., Yuan, L. and Li, Q. (2016). Polycyclic aromatic hydrocarbons (PAHs) in atmospheric $PM_{2.5}$, around 2013 Asian youth games period in Nanjing. *Atmos. Res.* 174–175: 85–96.

Li, X., Xia, X., Wang, L., Cai, R., Zhao, L., Feng, Z., Ren, Q. and Zhao, K. (2015). The role of foehn in the formation of heavy air pollution events in Urumqi, China. *J. Geophys. Res.* 120: 5371–5384.

Liao, C.M., Chio, C.P., Chen, W.Y., Ju, Y.R., Li, W.H., Cheng, Y.H., Liao, V.H.C, Chen, S.C and Ling, M.P. (2011). Lung cancer risk in relation to traffic-related nano/ultrafine particle-bound PAHs exposure: A preliminary probabilistic assessment. *J. Hazard. Mater.* 190: 150–158.

Lim, S., Vos, T. and Bruce, N. (2012). 'The burden of disease and injury attributable to 67 risk factors and risk factor clusters in 21 regions 1990-2010: A systematic analysis'. *Lancet* 380: 2224–2260.

Limu, Y.L.M.A.B.D., Lifu, D.L.N.T., Miti, A.B.L.Y., Wang, X. and Ding, X. (2013). Autumn and wintertime polycyclic aromatic hydrocarbons in $PM_{2.5}$ and $PM_{2.5\text{-}10}$ from Urumqi, China. *Aerosol Air Qual. Res.* 13: 407–414.

Liu, J., Man, R., Ma, S., Li, J., Wu, Q. and Peng, J. (2015). Atmospheric levels and health risk of polycyclic aromatic hydrocarbons (PAHs) bound to $PM_{2.5}$ in Guangzhou, China. *Mar. Pollut. Bull.* 100: 134–143.

Liu, X.G., Li, J., Qu, Y., Han, T., Hou, L., Gu, J., Chen, C., Yang, Y., Liu, X. and Yang, T. (2013). Formation and evolution mechanism of regional haze: A case study in the megacity Beijing, China. *Atmos. Chem. Phys.* 13: 4501–4514.

Maioli, O.L.G., Rodrigues, K.C., Knoppers, B.A. and Azevedo, D.A. (2010). Polycyclic aromatic and aliphatic hydrocarbons in Mytella charruana, a bivalve mollusk from Mundaú Lagoon, Brazil. *Microchem. J.* 96: 172–179.

Mantis, J., Chaloulakou, A. and Samara, C. (2005). PM_{10}-bound polycyclic aromatic hydrocarbons (PAHs) in the greater area of Athens, Greece. *Chemosphere* 59: 593–604.

Masih, A., Saini, R., Singhvi, R. and Taneja, A. (2010). Concentrations, sources, and exposure profiles of polycyclic aromatic hydrocarbons (PAHs) in particulate matter (PM_{10}) in the north central part of India. *Environ. Monit. Assess.* 163: 421–431.

Moon, H.B., Kannan, K., Lee, S.J. and Ok, G. (2006). Atmospheric deposition of polycyclic aromatic hydrocarbons in an urban and a suburban area of Korea from 2002 to 2004. *Arch. Environ. Contam. Toxicol.* 51: 494–502.

Niu, X., Ho, S.S.H., Ho, K.F., Huang, Y., Sun, J., Wang, Q. and Cao, J. (2017). Atmospheric levels and cytotoxicity of polycyclic aromatic hydrocarbons and oxygenated-PAHs in $PM_{2.5}$ in the Beijing-Tianjin-Hebei region. *Environ. Pollut.* 231: 1075–1084.

Okuda, T., Okamoto, K., Tanaka, S., Shen, Z., Han, Y. and Huo, Z. (2010). Measurement and source identification of polycyclic aromatic hydrocarbons (PAHs) in the aerosol in Xi'an, China, by using automated column chromatography and applying positive matrix factorization (PMF). *Sci. Total Environ*. 408: 1909–1914.

Park, S.U., Kim, J.G., Jeong, M.J. and Song, B.J. (2011). Source identification of atmospheric polycyclic aromatic hydrocarbons in industrial complex using diagnostic ratios and multivariate factor analysis. *Arch. Environ. Contam. Toxicol.* 60: 576–589.

Petry, T., Schmid, P. and Schlatter, C. (1996). The use of toxic equivalency factors in assessing occupational and environmental health risk associated with exposure to airborne mixtures of polycyclic aromatic hydrocarbons (PAHs). *Chemosphere* 32: 639–648.

Ravindra, K., Bencs, L., Wauters, E., De Hoog, J., Deutsch, F., Roekens, E. and Van Grieken, R. (2006). Seasonal and site-specific variation in vapour and aerosol phase PAHs over Flanders (Belgium) and their relation with anthropogenic activities. *Atmos. Environ*. 40: 771–785.

Ravindra, K., Sokhi, R. and Grieken, R. V. (2008). Atmospheric polycyclic aromatic hydrocarbons: Source attribution, emission factors and regulation. *Atmos. Environ*. 42: 2895–2921.

Ren, Y., Wang, G., Wu, C., Wang, J., Li, J., Zhang, L., Han, Y., Liu, L., Cao, C. and Cao, J. (2017). Changes in concentration, composition and source contribution of atmospheric organic aerosols by shifting coal to natural gas in Urumqi. *Atmos. Environ.* 148: 306–315.

Saha, M., Maharana, D., Kurumisawa, R., Takada, H., Yeo, G.B., Rodrigues, A.C., Bhattacharya, B., Kumata, H., Okuda, T. and He, K. (2017). Seasonal trends of atmospheric PAHs in five Asian megacities and source detection using suitable biomarkers. *Aerosol Air Qual. Res.* 17: 2247–2262.

Shi, J., Peng, Y., Li, W., Qiu, W., Bai, Z., Kong, S. and Jin, T. (2010). Characterization and source identification of PM_{10}-bound polycyclic aromatic hydrocarbons in urban air of Tianjin, China. *Aerosol Air Qual. Res.* 10: 507–518.

Simcik, M.F., Eisenreich, S.J. and Lioy, P.J. (1999). Source apportionment and source/sink relationships of PAHs in the coastal atmosphere of Chicago and Lake Michigan. *Atmos. Environ.* 33: 5071–5079.

Sosa, B.S., Porta, A., Lerner, J.E.C., Noriega, R.B. and Massolo, L. (2017). Human health risk due to variations in PM_{10}-$PM_{2.5}$ and associated PAHs levels. *Atmos. Environ.* 160: 27–35.

Tan, J.H., Bi, X.H., Duan, J.C., Rahn, K.A., Sheng, G.Y. and Fu, J.M. (2005). Seasonal variation of particulate polycyclic aromatic hydrocarbons associated with PM_{10} in Guangzhou, China. *Atmos. Res.* 80: 250–262.

Tao, M., Chen, L., Xiong, X., Zhang, M., Ma, P., Tao, J. and Wang, Z. (2014). Formation process of the widespread extreme haze pollution over northern China in January 2013: Implications for regional air quality and climate. *Atmos. Environ.* 98: 417–425.

Teixeira, E.C., Agudelo-Castañeda, D.M., Fachel, J.M.G., Leal, K.A., Garcia, K.D.O. and Wiegand, F. (2012). Source identification and seasonal variation of polycyclic aromatic hydrocarbons associated with atmospheric fine and coarse particles in the Metropolitan Area of Porto Alegre, RS, Brazil. *Atmos. Res.* 118: 390–403.

Teixeira, E.C., Garcia, K.O., Meincke, L. and Leal, K.A. (2011). Study of nitro-polycyclic aromatic hydrocarbons in fine and coarse atmospheric particles. *Atmos. Res.* 101: 631–639.

Tobiszewski, M. and Namieśnik, J. (2012). PAH diagnostic ratios for the identification of pollution emission sources. *Environ. Pollut.* 162: 110–119.

Tsai, P.J., Shieh, H.Y., Lee, W.J. and Lai, S.O. (2001). Health-risk assessment for workers exposed to polycyclic aromatic hydrocarbons (PAHs) in a carbon black manufacturing industry. *Sci. Total Environ*. 278: 137–150.

Wang, G., Huang, L., Zhao, X., Niu, H. and Dai, Z. (2006). Aliphatic and polycyclic aromatic hydrocarbons of atmospheric aerosols in five locations of Nanjing urban area, China. *Atmos. Res*. 81: 54–66.

Wang, G., Kawamura, K., Xie, M. and Hu, S. (2009). Size-distributions of n-hydrocarbons, PAHs and hopanes and their sources in the urban, mountain and marine atmospheres over East Asia. *Atmos. Chem. Phys.* 9: 8869–8882.

Wang, X., Cheng, H., Xu, X., Zhuang, G. and Zhao, C. (2008). A wintertime study of polycyclic aromatic hydrocarbons in $PM_{2.5}$ and $PM_{2.5\text{-}10}$ in Beijing: Assessment of energy structure conversion. *J. Hazard. Mater.* 157: 47–56.

Wu, D., Wang, Z., Chen, J., Kong, S., Fu, X., Deng, H., Shao, G. and Wu, G. (2014). Polycyclic aromatic hydrocarbons (PAHs) in atmospheric $PM_{2.5}$, and PM_{10}, at a coal-based industrial city: Implication for PAH control at industrial agglomeration regions, China. *Atmos. Res.* 149: 217–229.

Wu, Y., Wang, J., Liu, H., Lu, G.H. and Cui, X.H. (2008). Spatial distributions of atmospheric contaminations and effect of surface wind in Urumqi. *J. Desert Res.* 28: 986–991. (in Chinese)

Yang, X., Zhao, Y.Z., Li, Y.Y. and Zhao, K.M. (2009). Extreme weather events in Urumqi and their relation with regional climate change. *Arid Land Geogr.* 32: 867–873.

Yunker, M.B., Macdonald, R.W., Vingarzan, R., Mitchell, R.H., Goyette, D. and Sylvestre, S. (2002). PAHs in the Fraser River basin: A critical appraisal of PAH ratios as indicators of PAH source and composition. *Org. Geochem.* 33: 489–515.

Zhang, L., Chen, R. and Lv, J. (2016). Spatial and seasonal variations of polycyclic aeromatic hydrocarbons (PAHs) in ambient particulate matter (PM_{10}, $PM_{2.5}$) in three mega-cities in China and identification of major contributing source types. *Bull. Environ. Contam. Toxicol.* 96: 827–832.

Zhang, Y., Tao, S., Shen, H. and Ma, J. (2009). Inhalation exposure to ambient polycyclic aromatic hydrocarbons and lung cancer risk of Chinese population. *Proc. Natl. Acad. Sci. U.S.A.* 106: 21063–21067.

Zhou, J., Wang, T., Huang, Y., Mao, T. and Zhong, N. (2005). Size distribution of polycyclic aromatic hydrocarbons in urban and suburban sites of Beijing, China. *Chemosphere* 61: 792–799.

Received for review, May 7, 2018
Revised, July 22, 2018
Accepted, July 24, 2018